International Journal of Science and Research (IJSR)
ISSN (Online): 2319-7064
Index Copernicus Value (2015): 78.96 | Impact Factor (2015): 6.391

# Using Computational Fluid Dynamics to Evaluate the Impact of Convection Currents of Liquid Food for Simulating High Pressure Processing

**Abdul Ghani Albaali[1], Suhad S. Hussein[2]**

[1]Princess Sumaya University for Technology, Amman, Jordan

[2]Baghdad University, Baghdad, Iraq

**Abstract:** ***Temperature, velocity and pressure profiles during the early stages of high pressure compression of liquid food (water), within a three dimensional cylinder basket are simulated in this work. The computations domain was performed for a cylinder with a diameter of 38 mm and height of 290 mm, which are the same dimensions as those of the high pressure unit "FOOD-LAB model S-FL-850-9-W" used for measurements. Direct processing of water at pressure level of 500 MPa and a pressure holding time of 970s is simulated. Pressure is assumed to rise from atmospheric pressure to the treatment pressure linearly by enforced mass flow. The governing equations for continuity, momentum and energy conservation are solved using a commercial Computational Fluid Dynamics (CFD) package (PHOENICS), version 3.5, which is based on a finite volume method of solution. The objective of this research was to study the impact ofconvection currents. The simulation for the liquid food shows for the first time, the effect of forced and free convection flow, on the temperature distribution in the liquid at the early stages of compression. This is due to the difference between the velocity of the pumping fluid as it enters the cylinder inlet hole ($10^{-2}$ to $10^{-3}$) m/s and the velocity in the treatment chamber ($10^{-8}$-$10^{-9}$) m/s. Validation of the computed temperature at the different height at the axis of the cylinder are in a good agreement with those measured experimentally.***

**Keywords:** High pressure processing, CFD, Temperature distribution, Velocity profile

## 1. Introduction

High pressure processing (HPP) of foods is an investigated and proposed technology for high temperature short time commercial sterilization of chill and ambient stable low-acid food products (Knoerzer and Versteeg, 2009) HPP is of increasing interest because it permits microbial inactivation at low or moderate temperature with minimum degradation (Norton and Da-Wen Sun, 2008). Also, the energy required for compression is far less than that required in the thermal treatment. This type of treatment can be used not only for preservation but also for changing the physical and functional properties of foods. Non-thermal food processing using high pressure (HPP) can be applied to a large number of food products using batch or continuous treatment units. It has become clear in the last decade that high pressure processing may offer major advantages to the food preservation and processing industry (Barbosa-Canovas et al., 1997 and Ludikhuze et al., 1998).There is also a growing interest in the combined effects of temperature and pressure as an effective mean of inactivation of micro-organisms. Bacterial spores have more resistance to temperature and pressure than vegetative bacteria, and hence the combined pressure-thermal treatment must be applied for efficient deactivation of spores. HPP currently employs pressures of up to 700 MPa to increase the temperature of the preheated food to inactivate bacterial spores (Bull et al., 2009).

Heating caused by fluid compression can lead to a significant temperature distribution throughout the treated food. The inaccurate evaluation of this temperature variation would lead to the incorrect scale up of the high pressure processing units from laboratory size to industrial size. Moreover, if external heating is used to assist the HPP then the temperature distribution within the treatment chamber could be very significant. The development of a model to predict such a temperature distribution is very important, as experimental testing of every single food at different operating conditions can be time consuming.

The compression of a liquid system modifies its thermodynamic and fluid dynamic state and leads to a significant increase in the temperature of the compressed fluid, known as adiabatic heating. With external heating or cooling, temperature distribution within the treated volume will be always significant. This will lead to fluid density differences, which will induce a free convection heat transfer between the cylinder wall and the treated fluid. However,at the early stages of compression,the forced convection, caused by fluid entering the treatment chamber, strongly influences the temporal and spatial distribution of the temperature (Hartmann, 2002).

Computational Fluid Dynamics (CFD) models have been applied to different processing industries, such as the aerospace, automotive, nuclear and in the food processing applications. CFD models can be of great benefit in a variety of food engineering application; however it is only recently used in the application of high pressure processing (HPP) of foods.

There is a growing interest towards the use of mathematical models to predict the food temperature during the non-thermal treatment of foods such as the HPP, but literatures shows only limited attempts. A numerical simulation of thermo fluid-dynamic process during high-pressure treatment of food was studied by Hartman (2002). The simulation was conducted for water being compressed up to

500 MPa in a 4 ml chamber by enforced mass flow. The spatial and temporal evolution of temperature fields and fluid velocity fields were analyzed. The work shows that fluid motion is dominated by forced convection but only in the beginning of pressurizing. The temperature difference occurring in the high-pressure volume depends strongly on the pressure ramp during pressurization.

A numerical heat transfer model based on conduction during batch high hydrostatic pressure processing (HHP) of foods was analyzed for two food systems: apple sauce and tomato paste (Denys et al., 2000). Uniformity of inactivation of *Bacillus subtilis* α-amylase and soybean lipoxygenase during HPP processing was evaluated. The residual enzyme activity distribution appeared to be dependent on the inactivation kinetics of the enzyme under consideration and the pressure-temperature combination considered.

The influence of heat and mass transport effects on the uniformity of high-pressure induced inactivation was investigated by Hartman et al. (2003) through a numerical simulation. The inactivation of E. coli suspended in packed UHT milk carried out in a batch process with water as pressure medium is taken as a model process. The results show that, the inactivation rate increases with the geometrical scale of the high-pressure vessel. It is also shown than more than one log reduction in the residual surviving cell concentration can be observed depending on the package material and on the position and arrangement of the packages in the vessel (Hartman et al., 2003)

Hartman et al. (2004) studied the thermo fluid dynamics and process uniformity of HPP in a laboratory scale autoclave using experimental and numerical simulation techniques. Direct treatment of water at pressure levels of 500 MPa and 300 MPa was analyzed. It was found that maximum temperature differences at the end of the pressure holding phase (820 s) amount up to 6°C for high compression rate and 500 MPa target pressure. It was also noted that, the use of more viscous liquid leads to a substantial increase in the non-uniformity of temperature. The thermal insulation caused by the thick wall of the high-pressure chamber was found to be the key for providing high degree of uniformity.

In the present work, the non-adiabatic heating during high-pressure processing of food is analyzed by means of numerical simulations, at different periods of compression. Natural convection heating within a 3-D cylinder filled with water as a model liquid food during sterilization is simulated. Pressure is assumed to rise linearly from atmospheric pressure to the treatment pressure of 500 MPa. Unlike in the work reported in the literatures, the physical properties of liquid (water) were assumed to vary as the pressure increased during compression. Temperature, fluid velocity and pressure profiles within the model liquid are predicted and presented in a graphical form. The analysis of time and space dependant temperature in the liquid food at the early stages of pressure compression was the principle aims of this investigation. The effect of forced convection, velocity profile, temperature distribution and the shape of the hottest zone (HZ)during the compression were addressed in this paper.The work shows for the first time the effects of forced and natural convection current at early stages of compression during the high pressure processing.

## 2. Numerical Approximations and Model Parameters

High-pressure chamber of volume 300 ml is filled with liquid food (pure water)as shown in Fig. 1 in order to analyze the temperature distribution in the liquid during the high pressure treatment.The liquid food is compressed from ambient pressure to a maximum pressure of 500 MPa. The inflow of water is stopped when the maximum pressure is reached. The pressure level is held at 500 MPa for up to 1000 s. During the holding phase, the pressure remains constant. The initial temperature of the fluid and the wall temperature of the treatment chamber were assumed to be at 20°C during the whole period.

### 2.1 Computational Grid

A uniform grid system in radial and vertical directions is used in the simulation. The whole domain was divided into 5000 cells: 50 in radial direction and 100 in the vertical direction distributed equally in each direction. The computations domain was performed for a cylinder with a diameter (*D*) of 38 mm and height (*H*) of 290 mm. The geometry of high pressure chamber is constructed with the inlet at its top. Water was used as a model liquid food, compressed to 500 MPa in the 300 ml chamber for a period of 1000 s.

Different computational grids refinement study is used for the numerical solution of the governing equation to provide a mesh independent solution. Different inlet velocities are prescribed from the subroutine available in the software used for the simulation (PHOENICS). The velocity is ranging from $10^{-2}$-$10^{-3}$ m/s at the early stages of compression and decrease to very low values at the end of compression.

### 2.2 Governing Equations and Boundary Conditions

The partial differential equations governing natural convection of the fluid (water) being compressed and heated in a cylinder are Navier-Stokes equations given below (Bird et al., 1976).

***Energy conservation:***

$$\frac{\partial T}{\partial t}+v_r\frac{\partial T}{\partial r}+v_z\frac{\partial T}{\partial z}=\frac{k}{\rho C_p}\left[\frac{1}{r}\frac{\partial}{\partial r}\left(r\frac{\partial T}{\partial r}\right)+\frac{\partial^2 T}{\partial z^2}\right]+\frac{Q}{\rho C_p} \qquad (1)$$

where *Q* is the volumetric heat generation term due to adiabatic heating (i.e. source term) in $Wm^{-3}$.

***Momentum equation in the radial direction (r):***

$$\rho\left(\frac{\partial v_r}{\partial t}+v_r\frac{\partial v_r}{\partial r}+v_z\frac{\partial v_r}{\partial z}\right)=-\frac{\partial p}{\partial r}+\mu\left[\frac{\partial}{\partial r}\left(\frac{1}{r}\frac{\partial}{\partial r}(rv_r)\right)+\frac{\partial^2 v_r}{\partial z^2}\right] \quad (2)$$

***Momentum equation in the vertical direction (z):***

$$\rho\left(\frac{\partial v_z}{\partial t}+v_r\frac{\partial v_z}{\partial r}+v_z\frac{\partial v_z}{\partial z}\right)=-\frac{\partial p}{\partial z}+\mu\left[\frac{1}{r}\frac{\partial}{\partial r}\left(r\frac{\partial v_z}{\partial r}\right)+\frac{\partial^2 v_z}{\partial z^2}\right]+\rho g \quad (3)$$

These equations are coupled with the following equation:

***Continuity equation:***

$$\frac{\partial \rho}{\partial t}+\frac{1}{r}\frac{\partial}{\partial r}(r\rho v_r)+\frac{\partial}{\partial z}(\rho v_z)=0 \quad (4)$$

***The boundary conditions used were:***

At the cylinder boundary, $r = R$,

$$v_r=0,\ v_z=0,\ \mathrm{T}=20\ ^{\circ}\mathrm{C}\ \text{for}\ 0\le z\le H \quad (5)$$

At the bottom and top of the cylinder, $z = 0$ and $z = H$

$$v_r=0,\ v_z=0,\ \mathrm{T}=20^{\circ}\mathrm{C}\ \text{for}\ 0\le r\le R \quad (6)$$

$$At\ t=0,\ \ P=0.1\ MPa,$$
$$T=20^{\circ}C\ \ for\ \ 0\le r\le R\ and\ 0\le z\le H \quad (7)$$

$$At\ t\ge 0,\ P=16.663\ \ t+0.1\ MPa,$$
$$for\ 0\le r\le R\ and\ 0\le z\le H \quad (8)$$

$$At\ \ \ t>30\ \ s,\ \ P=500\ \ MPa \quad (9)$$

At the walls of the pressure chamber, the kinematic boundary condition requires zero fluid velocity, which implies a no slip condition. This assumption is valid except at the inlet.

### 2.3. Compression Steps

The pressure generated by the high pressure pump and intensifier of the HPP machine model S-FL-850-9-W used in this work, was found to increase with time linearly as shown in equation (8). After compression time of 30 s, the pressure remains constant at 500 MPa.

Simulations were conducted for time up to 1000 s and the results were presented when pressure reached 100, 200, 300, 400 and 500 MPa after 6, 12, 18, 24 and 30 s respectively. This was based on the performance of the high pressure processing unit, which was provided with a powerful pump. The pressure level of 500 MPa is reached within 30 s only. When the pressure reaches 500 MPa, it was held at that pressure until decompression starts. Reynolds number of the water flowing through the inlet hole is found small, therefore, the flow can be assumed laminar even at the beginning of the compression.

### 2.4. Physical Properties

An equation of state accounting for the compressibility of pure water under high pressure is implemented in the program to describe the variation of the density with pressure and temperature. This equation was taken from the study of Saul and Wagner (1989) as was implemented in one of the Phoenics subroutines used.

The properties of the model liquid food (water) at atmospheric pressure and ambient temperature of 20°C are: $\rho$ =998.23 kg $m^{-3}$, $C_P$ = 4181 $Jkg^{-1}K^{-1}$, $k$ = 0.597 $Wm^{-1}K^{-1}$ (Rahman, 1995 and Hayes,1987). As the pressure and temperature changes during compression, the program calculates the new values of physical properties, with the aid of FORTRAN statements written. The properties of water are calculated based on the updating values at every time step, which is done using the subroutines in PHOENICS, named CHEMKIN. A call is made to the CHEMKIN routine CKHMS to calculate these properties using the appropriate formula.

The liquid (water) is compressible under high pressure. Appropriate equations of state describing the density as a function of pressure and temperature have to be added to the equations as explained above.

The CHEMKIN system used for the liquid is supplied by Sandia National Laboratories and is consists of:

- A thermodynamics database.
- A library of FORTRAN subroutines which the user may call from his applications programmes to supply thermodynamic data.
- A "stand-alone" interpreter programme that reads a "plain language" file that specifies the thermodynamic data for the thermo-chemical system under investigation.

Associated with CHEMKIN, and also supplied by Sandia National Labs, is a further system that supplies transport data. The transport properties system consists of:

- A transport database.
- A library of FORTRAN subroutines which the user may call from his application programmes to supply viscosities, thermal conductivities, diffusion coefficients, and thermal diffusion ratios or coefficients calculated according to two approximations.
- A fitting programme that generates polynomial fits to the detailed transport properties in order to make the calculations performed by the subroutine library more efficient.

Another built in subroutine used in the simulation is named PRESS0, which is the parameter representing the reference pressure, to be added to the pressure computed by PHOENICS in order to give the physical pressure needed for calculating density and other physical properties. The use of this variable is strongly recommended in cases in which the static component of the pressure is much greater than the dynamic head. The reason is that the static component can be absorbed in PRESS0 leaving the stored pressure field, to represent the dynamic variations which otherwise may be lost in the round off, according to the machine precision and the ratio of dynamic pressure to the static head.

Several built in subroutines are used as well in this simulation, such as

- DVO1DT, used to calculate the volumetric coefficient of thermal expansion of the phase 1 of the material used (water). It is useful for the prediction of natural-convection heat transfer.
- DRH1DP, which is used to calculate the compressibility:

$$(\frac{d\rho 1}{dP})/\rho 1 \qquad ie.\frac{d(\ln \rho 1)}{dP} \qquad (10)$$

If DRH1DP given a positive value that value is used for the dependence of the first-phase density on pressure. Recourse to GROUND is necessary when density is a non-linear function of pressure, or a function of other variables. The following options have been provided in subroutine in PHOENICS called GXDRDP.

## 3. Results and Discussions

During high pressure processing of food, an increase of temperature due to compression is observed as a result of partial conversion of mechanical work into internal energy. This is known as adiabatic heating. In reality the situation is much more complex. In the simulation presented here, heat exchange between the treated fluid and the cylinder wall as well as the cooling effect caused by the entering fluid during compression is included in the analysis. Temperature distribution, location of the Hottest Zone (HZ), velocity profile and pressure profile during the process, are compared and analyzed based on the simulations conducted. Experimental measurements are used to validate these simulation results.

Fig.2 primarily shows the calculated pressure field, which shows the hydrostatic gradient (2.94 kPa at the base).The kinetic head is negligible due to the extremely low liquid velocity ($3x10^{-8}$ – $4x10^{-7}$ $ms^{-1}$) in the HP cylinder after such long time (1000 s), which can also shown in Fig.3.In order to minimize numerical errors, the pressure field solution calculates the pressure relative to that fixed at the inlet, which was increasing from atmospheric pressure to 500 MPa.

Figure 3 shows the velocity profile of the compressed fluid in the cylinder. The fluid adjacent to the external cooling at the wall will have higher density causing it to flow downward while at all other locations in the bulk of the cylinder, the liquid will flow upward. This can be shown clearly in Figure 3.The figure also shows that the velocity is in the range of $10^{-7}$ -$10^{-9}$ m/s at the end of the process. However at early stages of compression, the calculated liquid velocity was as high as $10^{-2}$-$10^{-4}$ m/s, as shown in Figures 4 and 5, after compression periods of 12 and 24 seconds respectively.

The changes in the temperature profile at early stages of compression is due to the compression heating and cooling caused by the pumped water through the hole at the top of the cylinder (inlet). The velocity of the cold water enter the inlet is much higher than the velocity inside the cylinder. It is in the range of $10^{-2}$-$10^{-3}$ m $s^{-1}$ compared to $10^{-8}$-$10^{-9}$ m $s^{-1}$inside the cylinder.At this stage, the buoyancy force starts to be effective due to temperature variation of the liquid from outside to the core of the cylinder.

Figures 4 and 5 show the temperature and velocity profiles at the early stages of compression after periods of 12 and 24 s at non-adiabatic compression pressures of 200 and 400 MPa respectively. Fig.4 shows that the fluid velocity at the top (location of the inlet) of the cylinder is large, which is in the range of $10^{-2}$- to $0^{-3}$ m/s at the top (at location close to the inlet) of the cylinder, while it is very small ($10^{-7}$- to $0^{-9}$ m/s) in the rest of cylinder as shown in Fig. 3. This is due to the liquid being pumped through the inlet at the top of cylinder in order to fill the shortage of water caused by the effect of compression. This will push the Hottest Heating Zone (HHZ) more toward the bottom of the cylinder as it's clearly seen in the figure. Without this effect, the HHZ will move more towards the top due to buoyancy effect.Fig. 5 shows that the fluid velocity is decreased to $10^{-3}$-$10^{-4}$ m/s at the top of the cylinder and remained very small in the rest of the cylinder, while the HHZis pushed even further towards the bottom of the cylinder.

Figure 6 shows temperature profile of the fluid due to non-adiabatic compression of 500 MPa after 1000 s of starting the compression. Due to the high hydrostatic pressure, the velocities are very small, and hence the effect of free convection heat transfer is expected to be very small in this situation. The HHZ (35.55$^{o}$C) after 30 s of no-adiabatic compression, which represents a 15$^{o}$C per 500 MPa, is almost at the center of the cylinder, with only very little shift toward the top of the cylinder. This is similar to the increase in temperature due to adiabatic heating usually reported in the literature (3$^{o}$C per 100 MPa). This figure shows that the increase in the fluid average temperature in the cylinder is significantly less than 3$^{o}$C, usually reported in adiabatic compression. The non-adiabatic condition occurs due to two factors: (1) cooling caused by the lower temperature of the wall of the cylinder; (2) cooling caused by the incoming fluid through the inlet of the cylinder.

Figs. 4, 5 and 6 shows for the first time the effects of forced and natural convection current at early stages of compression during the high pressure processing. At later stages of compression (Fig 3), the fluid flow diminishes and the liquid velocity drops to a very low values. Under such a condition heat transfer is more dominated by conduction and to less extent by free convection in the liquid.

### 3.1 Experimental Validation

The results of the simulation presented in this work were validated using experimental measurements. The experimental measurements are conducted using HPP unit model S-FL-850-9-W. The maximum operating pressure of the unit is 900 MPa and the operating temperature range is -20°C to + 90°C. The pressure vessel is fitted with 'T' type thermocouple at the axis of the vessel and can be adjusted to any position along the axis of the vessel.Pressure is controlled by electronic control module with integral digital display, with PLC (Mitsubishi 'F' series). The size of the HPP treatment cylinder is the same size as that used in the simulations, with a diameter of 38 mm and inner height of290 mm. Direct processing of water at pressure level of 500 MPa and within a pressure holding phase ending at 1000 s is considered.

Figures 8 and 9 show the measured and predicted temperature during the early stages of compression (t<30 seconds) at two different locations at the axis of the cylinder. The agreement is reasonable but that was possible only after the effect of cooling from the wall of the cylinder and by the entering fluid at the early stages of cooling. The effect of cooling by the entering fluid during compression is shown more clearly in Fig. 10. The temperature at the higher location is about 2°C lower than the center of the cylinder at the end of compression. If the cooling effect is ignored, the temperature at the higher location would experience higher temperature due to buoyancy.

In reality, a true isothermal operation is difficult to achieve. For HPP experiment at elevated temperatures, it's important to recognize that an externally delivered pressure-transmitting fluid may enter the system at a much lower temperature than the pressure-transmitting fluid already in the pressure vessel. The temperature of this fluid should be monitored and reported where possible (Balasubramaniam et al., 2004).

**Nomenclature**

| | |
|---|---|
| $C_p$ | specific heat of liquid food, J $kg^{-1}$ $K^{-1}$ |
| $D$ | diameter of cylinder, mm |
| $H$ | height of the cylinder, mm |
| $k$ | thermal conductivity of liquid food, W $m^{-1}$ $K^{-1}$ |
| $P$ | pressure, Pa |
| $Q$ | volumetric generation, W $m^{-2}$ |
| $r$ | radius of the cylinder, mm |
| $r, z$ | radial and vertical direction of the cylinder |
| $t$ | compressing time, s |
| $T$ | temperature, °C |
| $T_{ref}$ | reference temperature, °C |
| $v_r$ | velocity in radial direction, m $s^{-1}$ |
| $v_z$ | velocity in vertical direction, m $s^{-1}$ |
| $\beta$ | thermal expansion coefficient, $K^{-1}$ |
| $\mu$ | apparent viscosity, Pa s |
| $\rho$ | density, kg $m^{-3}$ |
| $\rho_{ref}$ | reference density, kg $m^{-3}$ |

## 3. Conclusions

Numerical simulation of non-adiabatic compression of liquid food (water) has been conducted using finite volume method analysis. Physical properties of liquid were introduced into the simulation program as a function of both temperature and pressure. The simulation shows for the first time the effect of forced convection heat transfer on the temperature distribution of liquid at the early stages of compression, which is caused by the flow of the pressure transmitting liquid into the cylinder. The simulation also shows the effect of the free convection currents,induced by the temperature difference, on the location of the hottest region at the early times of compression.

## References

[1] Barbosa-Canovas, G.V., Pothakamury, U.R., Paulo, E. and Swanson, B.G. (1997). Non Thermal Preservation of Foods, New York: Decker. P 9-52.
[2] Balasubramaniam, V. M., Ting, E. Y., Stewart, C. M., and Robbins, J. A. (2004). Recommended laboratory practise for conducting high pressure microbial inactivation experiments. *Journal of Innovative Food Science and Emerging Technologies*, 5(2004) 299-306.
[3] Bird, R.B., Stewart, W.E., and Lightfoot, E.N. (1976). Transport Phenomena, John Wiley and Sons, New York.
[4] Bull, M.K., Olever, S.A., and Chapman, B. (2009). Synergistic inactivation of *Clostridium botulinum* spores by high pressure and heat is strain and product dependent, *Applied and Environmental Microbiology*, 75(2), 434-445.
[5] Denys, S., Van Loey, A. M., &Hendrickx, M. E. (2000). A modeling approach for evaluating process uniformity during batch high hydrostatic pressure processing: combination of a numerical heat transfer model and enzyme inactivation kinetics. *Journal of Innovative Food Science & Emerging Technologies*, 1, 5-19.
[6] Ghani, A. G., Farid, M. M., and Richards, P. A simulation study of heat transfer during high pressure processing of food using computational fluid dynamics (CFD). CHEMECA 2004 Conference, Sydney, Australia.
[7] Hartman, C., Schuhholz, J. P., Kitsubun, P., Chapleau, N., Bali, A. L., & Delgado, A. (2004). Experimental and numerical analysis of thermofluiddynamics in a high-pressure autoclave. *Journal of Innovative Food Science & Emerging Technologies*, 5, 399-411.
[8] Hartmann, Chr., Delgado, A., &Szymczyk, J. (2003). Convective and diffusive transport effects in a high pressure induced inactivation process of packed food, *Journal of Food Engineering*, 59, 33-44.
[9] Hartmann, Chr. (2002). Numerical simulation of thermodynamic and fluid-dynamic processes during high-pressure treatment of fluid food system. *Journal of Innovative Food Science and Emerging Technologies*, 3(2002) 11-18.
[10] Hayes (1987). Food Engineering Data Handbook, John Wiley & Sons Inc., New York, NY10158.
[11] Kai Knoerzer and CornelisVersteeg. (2009). A CFD model for simulating high pressure thermal (HPT) processing-Impact of material properties and processing conditions on prediction accuracy. Seventh International Conference on CFD in the Minerals and Process

Industries, CSIRO, Melbourne, Australia, 9-11 December 2009.
[12] Ludikhuyze, L., Indrawati, I., Van der Broeck, C., Weemens, C., and Hendrickx, M.E. (1998). Effect of combined pressure and temperature on soybean lipoxygenase . 2. Modeling inactivation kinetics under static and dynamic conditions. *Journal of Agricultural food Chemistry*, 46, 4081-4086.
[13] Rahman, R. (1995). *Food Properties Handbook*. CRC Press, Inc., U.S.A.
[14] Saul, A., & Wagner, w. (1989). A fundamental equation for water covering the range from the melting line to 1273 K at pressures up to 25000 MPa, *Journal of Physical and Chemical Reference Data*, 9, 1212-1255.
[15] Scott, G., & Richardson, P. (1997). The applications of computational fluid dynamics in the food industry. *Journal of Trends in Food Science & Technology*, 8, 119-124.
[16] Tomás Norton & Da-Wen Sun. (2008). Recent advances in the use of high pressure as an effective processing technique in the food industry. *Food Bioprocess Technology*,1:2–34. DOI 10.1007/s11947-007-0007-0

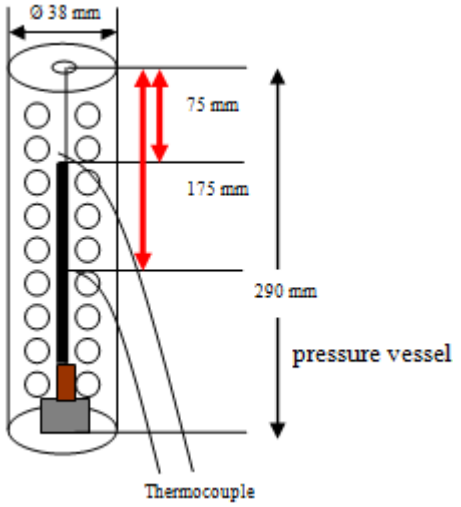


**Figure 1:** Geometry of the high pressure vessel.

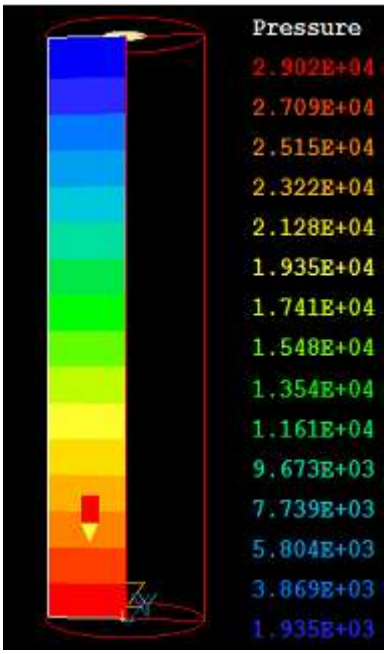


**Figure 2:** Pressure variation in the fluid along the cylinder height (1000 s, P=500 MPa)

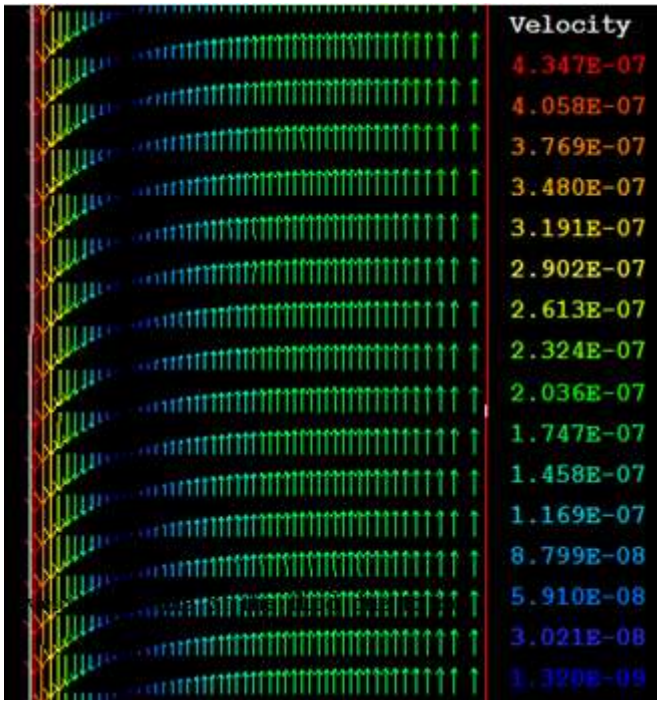


**Figure 3:** Enlarged section of velocity profile of the fluid due to no-adiabatic compression (t=1000 s, P=500 MPa)

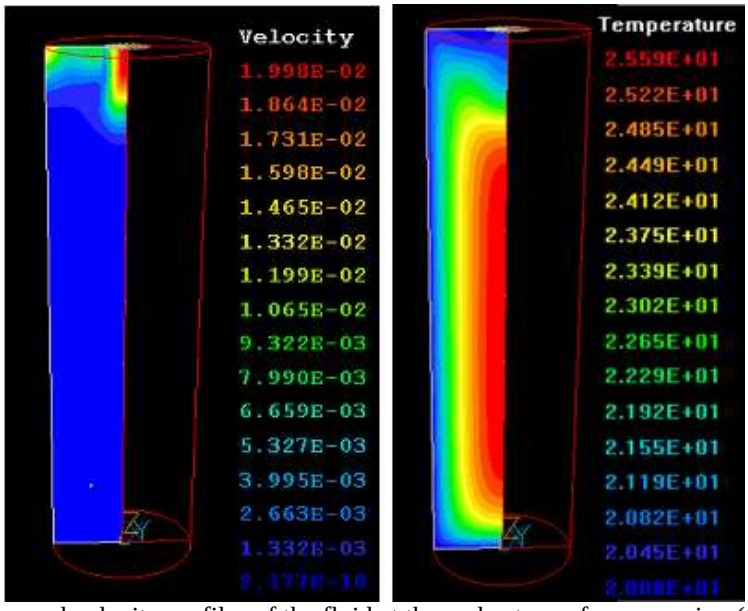


**Figure 4:** Temperature and velocity profiles of the fluid at the early stage of compression (t=12 s, P=200 MPa).

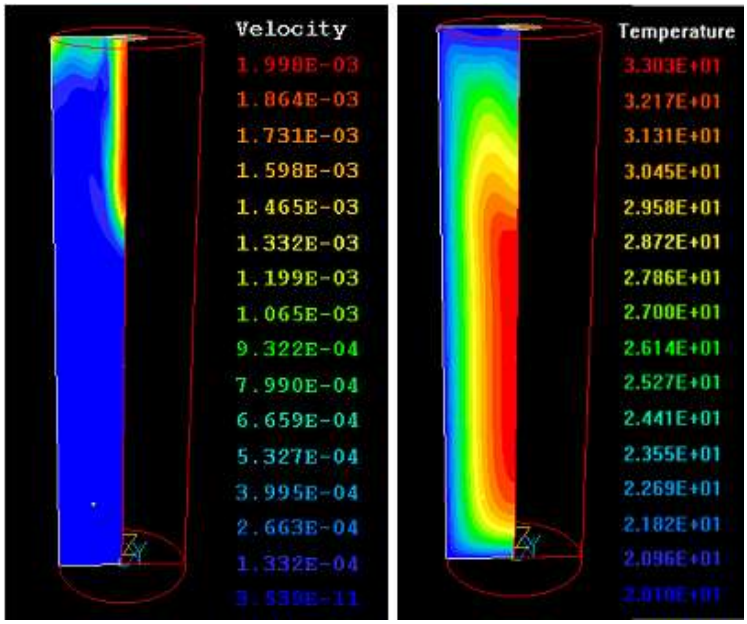


**Figure 5:** Temperature and velocity profiles of the fluid at the early stage of compression (t=24 s, P=400 MPa).

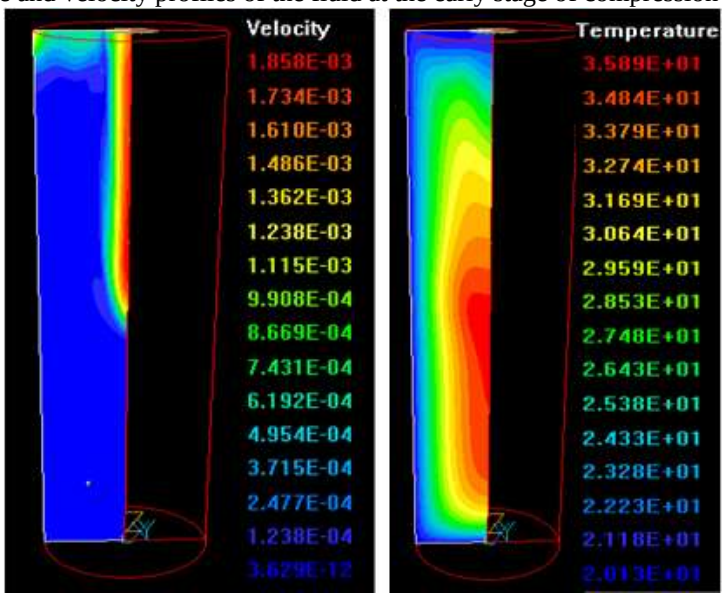


**Figure 6:** Temperature and velocity profiles of the fluid at the early stage of compression (t=30 s, P=500 MPa).

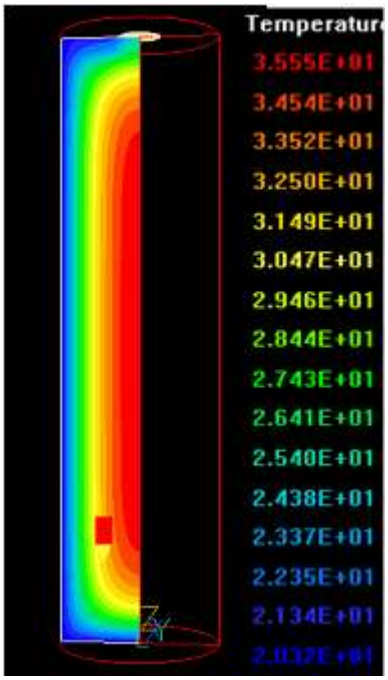


**Figure 7:** Temperature profile of the fluid due to non-adiabatic compression (t = 1000 s, P = 500 MPa).

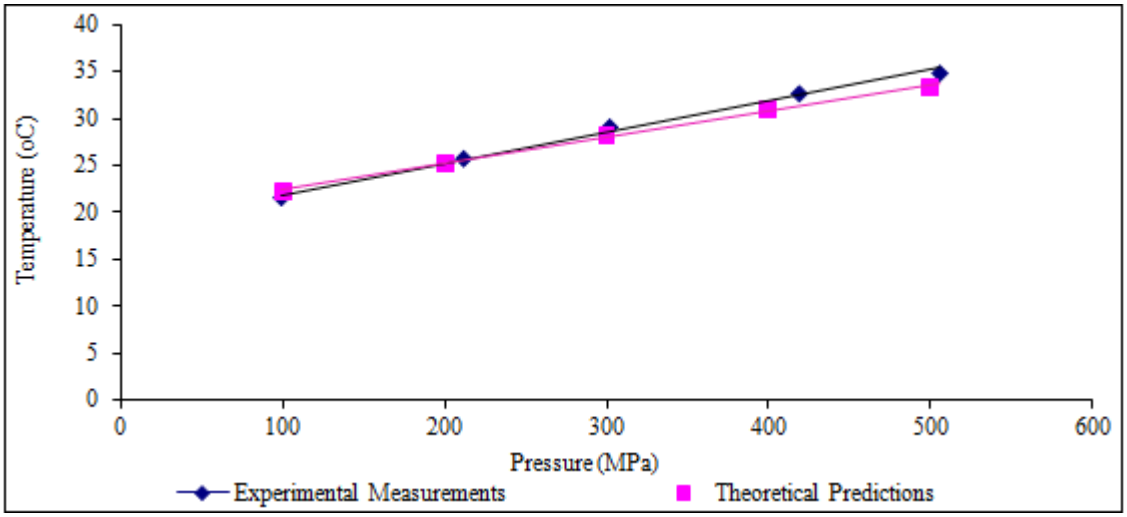


**Figure 8:** Experimental measurements and theoretical predictions of temperature of a liquid food (water) at the center of pressure vessel, 75 mm from its top

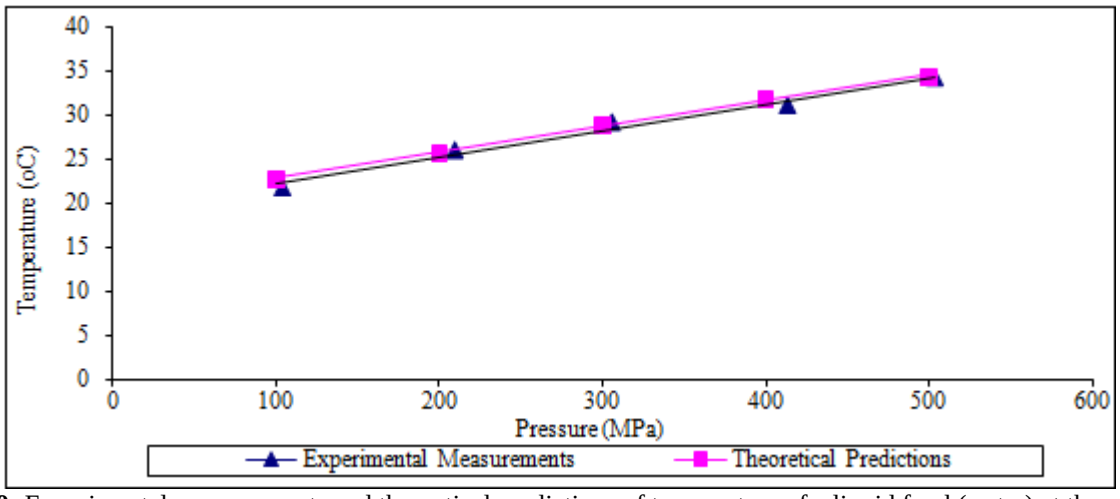


**Figure 9:** Experimental measurements and theoretical predictions of temperature of a liquid food (water) at the center of pressure vessel, 175 mm from its top

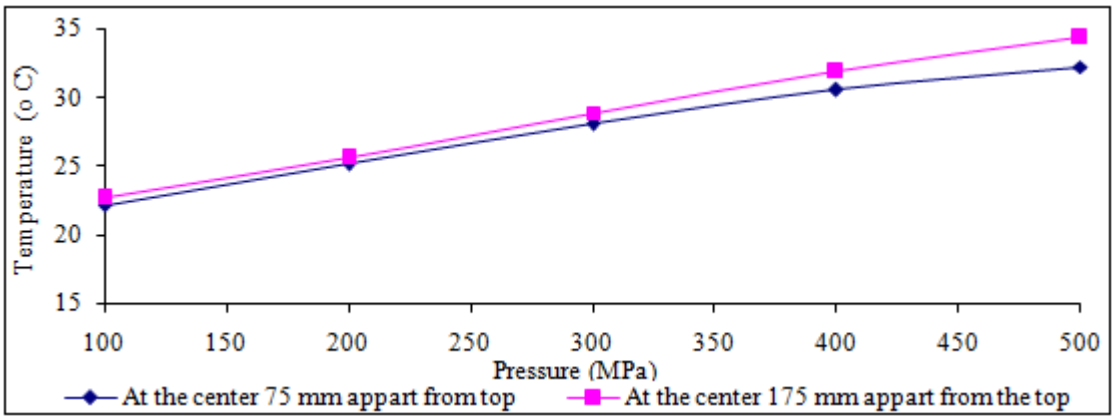


**Figure 10:** Comparison between 2 theoretically predicted points at different heights; top point located at the center of the pressure vessel 75 mm from top.